

# Self-Similar Collapse of Nonrotating Magnetic Molecular Cloud Cores

Ioannis Contopoulos,<sup>1</sup> Glenn E. Ciolek, and Arieh Königl

Department of Astronomy and Astrophysics, University of Chicago  
5640 S. Ellis Avenue, Chicago, IL 60637

Accepted for publication in *The Astrophysical Journal*, 1 Sept 1998 issue

## ABSTRACT

We obtain self-similar solutions that describe the gravitational collapse of nonrotating, isothermal, magnetic molecular cloud cores. We use simplifying assumptions but explicitly include the induction equation, and the semianalytic solutions we derive are the first to account for the effects of ambipolar diffusion following the formation of a central point mass. Our results demonstrate that, after the protostar first forms, ambipolar diffusion causes the magnetic flux to decouple in a growing region around the center. The decoupled field lines remain approximately stationary and drive a hydromagnetic C-shock that moves outward at a fraction of the speed of sound (typically a few tenths of a kilometer per second), reaching a distance of a few thousand AU at the end of the main accretion phase for a solar-mass star. We also show that, in the absence of field diffusivity, a contracting core will not give rise to a shock if, as is likely to be the case, the inflow speed near the origin is nonzero at the time of point-mass formation. Although the evolution of realistic molecular cloud cores will not be exactly self similar, our results reproduce the main qualitative features found in detailed core-collapse simulations (Ciolek & Königl 1998).

*Subject headings:* accretion, accretion disks — diffusion — ISM:clouds — ISM: magnetic fields — MHD — stars: formation

---

<sup>1</sup>Present address: Physics Department, University of Crete, P. O. Box 2208, Heraklion 71003, Greece

## 1. Introduction

Low-mass stars are generally believed to form as a result of the gravitational collapse of molecular cloud cores. The cores are initially supported by thermal and magnetic forces, but because of ambipolar diffusion (the drift of ions, to which the magnetic field lines are attached, relative to the dominant neutral gas component), they gradually lose their magnetic support and eventually collapse after becoming “supercritical” (see, e.g., Mouschovias 1987 for a review).<sup>2</sup> The most detailed numerical treatments to date of the problem of the ambipolar diffusion-initiated formation of supercritical cores and the early stages (prior to point mass formation) of their subsequent dynamical collapse have been presented by Mouschovias and collaborators (Fiedler & Mouschovias 1992, 1993; Ciolek & Mouschovias 1993, 1994, 1995, hereafter CM93, CM94, CM95; Basu & Mouschovias 1994, 1995a, 1995b, hereafter BM94, BM95a,b). Because the timescale for core formation is much longer than the timescale for dynamical collapse, special numerical techniques had to be employed in these calculations. The simulations were terminated when the central densities reached  $\sim 10^{10}$  cm $^{-3}$  and the underlying assumptions of isothermality (e.g., Gaustad 1963) and flux freezing onto the ions (e.g., Pneuman & Mitchell 1965) broke down. These calculations were nevertheless able to demonstrate that *supercritical cores begin to collapse dynamically before a point mass (i.e., a protostar) appears at the origin*.

The dynamical evolution of supercritical cores after their formation has been studied by many researchers. Solutions exist for the collapse of nonrotating, self-gravitating spheres without thermal support (Henriksen 1994), self-gravitating spheres with thermal support (Penston 1969; Larson 1969; Shu 1977; Hunter 1977; Boss & Black 1982; Whitworth & Summers 1985; Foster & Chevalier 1993) as well as with a combined thermal and isotropic magnetic pressure support (Chiueh & Chou 1994), and self-gravitating disks with thermal support (Narita, Hayashi, & Miyama 1984; Matsumoto, Hanawa, & Nakamura 1997) and also with ordered, frozen-in magnetic fields (Nakamura, Hanawa & Nakano 1995; Li & Shu 1997, hereafter LS). In order to choose a particular solution for a given problem, one needs to know the properties of the supercritical core at the time of its formation. This information, however, can only be gleaned from a study of the preceding, quasi-static evolution of the core under the influence of ambipolar diffusion. Although different assumptions about the initial state of the core yield solutions that are qualitatively similar in their gross behavior (the core collapses with near free-fall speeds and a point mass eventually forms at the center), the solutions do differ in such important details as the

---

<sup>2</sup>In this paper we reserve the term “core” for the high-density central region of a molecular cloud and do *not* apply it to the point mass that forms from the collapse of such a core.

accretion rate onto the central point mass and the formation (or absence) of shocks.

The well-known examples of the Larson-Penston (1969) and Shu (1977) similarity solutions in fact represent two extremes of a whole continuum of self-similar collapse solutions specified by a cloud’s initial configuration and the conditions at its boundary (Hunter 1977; Whitworth & Summers 1985; see also Chiueh & Chou 1994 for a generalization to the case of an isotropic internal magnetic pressure). The Larson-Penston (1969) solution is characterized by a spatially uniform, supersonic (at  $\sim 3.3$  times the isothermal speed of sound  $C$ ) infall speed and an inverse-square dependence of the density  $\rho$  on the radius  $r$  at the instant of point-mass formation (PMF); the mass accretion rate at the center is  $\sim 29 C^3/G$  (where  $G$  is the gravitational constant) at that instant and increases to  $\sim 47 C^3/G$  immediately after PMF. Numerical simulations of the collapse of nonmagnetic isothermal spheres (Hunter 1977; Foster & Chevalier 1993) have indicated that this solution provides a good approximation to the conditions near the center at the PMF epoch for clouds that are initially near a marginally stable equilibrium. The Shu (1977) solution strictly applies only to the post-PMF evolutionary phase: it consists of an inner free-fall region and a hydrostatic outer envelope that are separated by an outward-propagating (at a speed  $C$  relative to the gas) expansion wave. The envelope corresponds to a singular isothermal sphere ( $\rho \propto r^{-2}$ ) and the mass accretion rate onto the center is  $\sim 1 C^3/G$ . In applying this solution to real systems, it was proposed to identify the initial core configuration at the end of the quasi-static ambipolar-diffusion phase with a singular isothermal sphere (or, more generally, a toroid) at the instant of PMF (e.g., Shu, Adams, & Lizano 1987; Li & Shu 1996). However, as we noted above, the conclusion from detailed numerical simulations has been that the dynamical phase of core collapse generally commences well before the PMF epoch, so that the innermost region is not well represented by a quasi-static solution at the time of point-mass formation.

Another interesting effect that depends on the specific choice of initial conditions and on the detailed physical properties of the collapsing core is the formation (or absence) of shocks (e.g., Tsai & Hsu 1995; LS). For example, LS discovered that when, instead of a spherical core, one considers the collapse of a flattened disk, the expansion wave of Shu (1977) becomes a shock. As we show in this paper, when one takes proper account of the fact that supercritical cores collapse dynamically before a point mass first forms at the origin, that shock disappears. Nevertheless, a physical basis for the formation of shocks in collapsing magnetized molecular cloud cores has been discussed by Li & McKee (1996), who argued that a hydromagnetic C-shock will appear as a result of the outward diffusion of inwardly advected magnetic flux. The existence of such a shock has been confirmed in the numerical simulations of Ciolek & Königl (1998, hereafter CK), and it is, in fact, a salient feature of the semianalytic solutions derived in this paper.

The aim of the present work is to clarify the effects of ambipolar diffusion in dynamically collapsing supercritical cores. Toward this goal, we construct semianalytic, time-dependent similarity solutions of gravitationally contracting, magnetized, isothermal disks. Although the evolution of real molecular cloud cores is not expected to be exactly self similar, we demonstrate, through a comparison with the detailed numerical simulations of CK, that our solutions capture the main traits exhibited by the latter calculations. Based on an analogous comparison with the results of numerical simulations, Basu (1997) showed that a self-similar scaling describes the pre-PMF evolution in the innermost flux tubes of collapsing supercritical cores quite well. To complement his study, we concentrate in this paper on the post-PMF evolutionary phase. Our approach differs, however, from that of Basu (1997) in that we explicitly solve the induction equation, whereas he accounted for the effects of ambipolar diffusion only in a phenomenological manner.<sup>3</sup> In fact, the solutions that we derive, while involving various simplifications, are nevertheless the first to consistently incorporate ambipolar diffusion into a self-similar representation of the collapse of a magnetized cloud core.<sup>4</sup> We formulate the problem in §2, present our solutions in §3, and discuss the results in §4. Our conclusions are summarized in §5.

## 2. Mathematical Formulation and Approximations

The problem of the self-initiated formation and contraction of cloud cores due to ambipolar diffusion in axisymmetric, self-gravitating, isothermal, magnetic molecular clouds was formulated in detail in CM93. In the presence of an ordered, large-scale magnetic field the contracting cloud core assumes a disk-like configuration on account of the fact that the magnetic stresses inhibit motion normal to the field lines (see Fiedler & Mouschovias 1993). Along the field lines it is a good approximation to assume that the cloud is at all times in hydrostatic equilibrium, with thermal pressure providing support against vertical gravity. For simplicity, we neglect both the pressure support provided by internal hydromagnetic waves (i.e., “turbulence”) and the vertical squeezing of the core by the external thermal

---

<sup>3</sup>Our work is thus also distinguished from that of Safier, McKee, & Stahler (1997), who studied the effects of ambipolar diffusion in the spherically symmetric, quasi-static limit without explicitly solving the induction equation.

<sup>4</sup>The effect of *weak* magnetic fields on a dynamically collapsing core in the presence of ambipolar diffusion was previously investigated by Galli & Shu (1993a), who carried out a perturbation expansion of the (nonmagnetic) spherical similarity solution of Shu (1977). As was already noted and discussed by Li & McKee (1996), the semianalytic solution derived in that paper, as well as the associated numerical calculation in Galli & Shu (1993b), did not uncover the existence of a flux diffusion-driven shock.

and magnetic pressure (including, in particular, the squeezing induced by the radial field component at the disk surface; see eq. [9] in CK). For a self-gravitating disk with possibly a point mass at the center, the hydrostatic balance equation can thus be written as

$$\rho C^2 = \frac{\pi}{2} G \sigma^2 + \frac{GM_c \rho h^2}{2r^3} , \quad (1)$$

where  $r$  is the cylindrical radius,  $\sigma$  is the surface density,  $\rho$  is the gas density,  $h \equiv \sigma/2\rho$  is the vertical scale height (assumed to be  $\ll r$ ),  $C = (k_B T/m_n)^{1/2}$  is the isothermal speed of sound (with  $k_B$  being the Boltzmann constant,  $T$  the temperature, and  $m_n$  the mean mass of a gas particle), and  $M_c$  is the mass of the star that forms at the center. Equation (1) implies that

$$h = \begin{cases} rC(GM_c/2r)^{-1/2} & \text{near the central point mass} \\ C^2[\pi G \sigma]^{-1} & \text{far from the central point mass} \end{cases} . \quad (2)$$

The collapse of the core can be described using the mass and (radial) momentum conservation equations, which, in cylindrical coordinates  $(r, \phi, z)$ , read

$$\frac{\partial \sigma}{\partial t} + \frac{1}{r} \frac{\partial}{\partial r} (r \sigma u) = 0 \quad (3)$$

and

$$\frac{\partial u}{\partial t} + u \frac{\partial u}{\partial r} = g_r - C^2 \frac{\partial \ln \sigma}{\partial r} + \frac{B_z}{2\pi\sigma} \left( B_{r,s} - h \frac{\partial B_z}{\partial r} \right) , \quad (4)$$

respectively. Here  $B_{r,s}$  is the radial component of the magnetic field at the surface of the thin disk (by symmetry,  $B_r = 0$  at the midplane  $z = 0$ , and  $\partial B_r / \partial z \approx B_{r,s}/h$ ),  $u$  is the radial velocity component, and  $g_r$  is the radial component of the gravitational acceleration. As is well known, the calculation of  $g_r$  for a self-gravitating thin disk is in general nontrivial. The above equations are supplemented by the induction equation for the magnetic field (see derivation below),

$$\frac{\partial \Psi}{\partial t} = -2\pi r \left[ u B_z + C \frac{\eta}{\lambda^2} \left( \frac{\pi G \sigma h}{C^2} \right)^{1/2} \left( B_{r,s} - h \frac{\partial B_z}{\partial r} \right) \right] , \quad (5)$$

where

$$\eta \equiv \tau_{ni} / (8\pi G \rho)^{-1/2} \approx 0.7 \xi_{-17}^{-1/2} , \quad (6)$$

the ratio of the mean collision time  $\tau_{ni}$  of a neutral particle with a sea of ions and the approximate free-fall time due to the disk self-gravity, is a measure of the efficiency of ambipolar diffusion in the disk, and

$$\lambda \equiv \frac{2\pi G^{1/2} \sigma}{B_z} \quad (7)$$

is the dimensionless local mass-to-flux ratio. In equation (5)  $\Psi(r, t) \equiv \int_0^r 2\pi r' B_z(r', t) dr'$  is the magnetic flux threading the disk interior to the radius  $r$  at time  $t$ , whereas in equation (6)  $\xi = 10^{-17} \xi_{-17} \text{ s}^{-1}$  is the cosmic-ray ionization rate per hydrogen nucleus (e.g., Watson 1976). In deriving equation (5) we have assumed that the disk is weakly ionized and that the magnetic field is “frozen” into the ions (valid for disk densities  $\lesssim 10^{11} \text{ cm}^{-3}$ ). The first assumption implies

$$\rho_i \ll \rho_n , \quad (8)$$

where the subscripts  $i$  and  $n$  refer, respectively, to the ions and neutrals. Under this assumption, one can identify  $\rho$  in the preceding equations with  $\rho_n$ , and  $u$  with  $u_n$ . The speeds  $u_n$  and  $u_i$  are not, in general, equal, and their difference  $u_D \equiv (u_i - u_n)$  is referred to as the (radial) ion–neutral drift speed. The second assumption can be expressed by writing the flux conservation equation in the form

$$\frac{\partial \Psi}{\partial t} = -2\pi r u_i B_z = -2\pi r (u_n + u_D) B_z . \quad (9)$$

Magnetic forces that act on the ions are transferred to the neutrals through a collisional drag force,

$$\frac{\rho u_D}{\tau_{ni}} = \frac{B_z}{4\pi} \left( -\frac{\partial B_z}{\partial r} + \frac{\partial B_r}{\partial z} \right) . \quad (10)$$

For a disk that consists of a molecular hydrogen gas with a helium number density that is 10% of the density of hydrogen nuclei, the neutral–ion mean collision time is given by  $\tau_{ni} = 1.4(m_i + m_{H_2})/[\rho_i \langle \sigma w \rangle_{iH_2}]$ , where  $\langle \sigma w \rangle_{iH_2} = 1.69 \times 10^{-9} \text{ cm}^3 \text{ s}^{-1}$  is the average collisional rate between ions and hydrogen molecules (e.g., McDaniel & Mason 1973). By balancing ionization by cosmic rays with dissociative recombination, one can express the ion number density as  $n_i \approx (\xi n / a_{\text{dr}})^{1/2}$  (Elmegreen 1979), where  $a_{\text{dr}} \approx 10^{-6} \text{ cm}^3 \text{ s}^{-1}$  is the electron dissociative recombination rate (e.g., Dalgarno 1987) and  $n$  is the neutral particle number density. Although this expression (which was used in deriving the dependence of  $\eta$  on  $\xi$  in eq. [6]) is strictly valid only for densities  $n \lesssim 10^6 \text{ cm}^{-3}$  (at densities  $\gg 10^6 \text{ cm}^{-3}$ ,  $n_i \approx \text{const}$ ; see Figs. 2c and 4c in CM94, and Figs. 1 – 3 in Ciolek & Mouschovias 1998), we nevertheless adopt it in this paper for all disk densities since it allows us to obtain a self-similar set of equations that can be directly integrated. Equation (5) follows from combining equations (9) and (10) and taking the ion mass to be  $m_i = 29 m_H$ . Equation (10) brings out the well-known fact that, in order to support a nonuniform magnetic field distribution in the disk, the ion–neutral drift speed has to be nonzero. We return to this basic point in §3.1.

Given the distributions  $\sigma(r, 0)$ ,  $u(r, 0)$ , and  $B_z(r, 0)$  at some initial time  $t = 0$ , one can in principle integrate equations (3)–(5) provided that  $g_r(r, t)$  and  $B_{r,s}(r, t)$  can be expressed as functions of  $\sigma$  and  $B_z$ , respectively. In the limit of a thin disk with negligible mass

outside, one can obtain the radial gravitational acceleration at radius  $r$  by adding the contributions from rings of disk material at all radii  $r'$ ,

$$g_r(r, t) = -\frac{G}{r^2} \int_0^\infty 2\pi r' \sigma(r', t) \mathcal{R}(r'/r) dr' . \quad (11)$$

In this equation,

$$\mathcal{R}(X) = \frac{1}{2\pi} \int_0^{2\pi} \frac{(1 - X \cos \phi) d\phi}{(1 + X^2 - 2X \cos \phi)^{3/2}} = \mathcal{K}(X) + X \frac{d\mathcal{K}}{dX} , \quad (12)$$

where

$$\mathcal{K}(X) \equiv \frac{2}{\pi(1 + X)} K(4X/[1 + X]^2) , \quad (13)$$

with  $K(x)$  being the complete elliptic integral of the first kind (see CM93). Figure 1 shows a plot of  $\mathcal{R}(X)$  obtained using approximate formulas for  $K(x)$  (e.g., Abramowitz & Stegun 1965, p. 591). It is seen that contributions to the gravitational acceleration at a radius  $r$  arise from disk material both interior *and* exterior to  $r$ . There exist, however, two limits in which the simple expression

$$g_r = -\frac{GM}{r^2} \quad (14)$$

holds true, where  $M(r, t) \equiv \int_0^r 2\pi r' \sigma(r', t) dr'$  is the mass interior to the radius  $r$  at time  $t$ : (a) when  $\sigma \propto r^{-1}$ , and (b) when the gravitational pull of a point mass at the center dominates over the disk self-gravity. As we demonstrate below, equation (14) is a very good approximation to the true value of  $g_r$  during the post-PMF phase of the disk evolution. For future reference, we note here that the mass conservation equation (3) can be rewritten in terms of  $M(r, t)$  in the form

$$\frac{\partial M}{\partial t} + u \frac{\partial M}{\partial r} = 0 . \quad (15)$$

What about  $B_{r,s}$ ? Assuming that the medium surrounding the disk is current-free, the magnetic field can be expressed as the gradient of a potential:  $\mathbf{B} = \nabla\Phi$ . Now, since  $\nabla \cdot \mathbf{B} = 0$ , this scalar potential satisfies Laplace's equation

$$\nabla^2\Phi = 0 \quad (16)$$

with Neumann boundary conditions

$$\frac{\partial\Phi}{\partial z} = \begin{cases} B_z & \text{at the surface of the disk } (z \simeq 0) \\ B_{z,\infty} & \text{at infinity} \end{cases} ,$$

where  $B_{z,\infty}$  is the uniform and constant large-scale magnetic field that is frequently observed to thread molecular clouds on scales that are large in comparison with their (flattened) inner

cores (e.g., Hildebrand, Dragovan, & Novak 1984; Novak, Predmore, & Goldsmith 1990; Kane et al. 1993). Therefore, in the ideal case of a current-free medium outside a thin disk, the function  $\Phi - zB_{z,\infty}$  satisfies the same equation and (Neumann) boundary conditions as the gravitational potential  $V$  (where  $\mathbf{g} = -\nabla V$ ,  $\nabla^2 V = 0$ ,  $\partial V/\partial z = 2\pi G\sigma$  at  $z = 0$ , and  $\partial V/\partial z = 0$  at infinity). Hence, by direct analogy with the expression for  $g_r$  in equation (11), one can write

$$\begin{aligned} B_{r,s}(r, t) &\equiv \frac{\partial \Phi}{\partial r} \Big|_{z=0} \\ &= \frac{\partial}{\partial r} (\Phi - zB_{z,\infty}) \Big|_{z=0} \\ &= \frac{1}{r^2} \int_0^\infty r' (B_z(r', t) - B_{z,\infty}) \mathcal{R}(r'/r) dr' \end{aligned} \quad (17)$$

$$\approx \frac{1}{r^2} \int_0^\infty r' B_z(r', t) \mathcal{R}(r'/r) dr' , \quad (18)$$

where the last approximation is valid when  $B_z$  at the disk surface is  $\gg B_{z,\infty}$  (see CM93, CM94, CM95, BM94, and BM95a,b). When one considers *only* the inner parts of the collapsing disk, as in the present analysis, one can neglect  $B_{z,\infty}$ .<sup>5</sup> Pursuing the analogy with gravity even further, one sees that it is possible to use the simple expression

$$B_{r,s} = \frac{\Psi}{2\pi r^2} \quad (19)$$

when either (a)  $B_z \propto r^{-1}$  or (b) the magnetic field advected to the center can be represented by a split monopole that dominates over the disk magnetic field. We will demonstrate that either (a) or (b) are applicable in a collapsing disk following the formation of a central point mass, so that equation (19) provides a good approximation to  $B_{r,s}$  during that phase.

### 3. Self-Similar Solutions

#### 3.1. The “Pivotal” State

Although one can in principle integrate equations (3)–(5) for any set of physically reasonable initial conditions [expressed by the functions  $\sigma(r, 0)$ ,  $u(r, 0)$ , and  $B_z(r, 0)$ ], one particular set of initial distributions makes it possible to obtain self-similar solutions that

---

<sup>5</sup>When the strong inequality  $B_z \gg B_{z,\infty}$  no longer holds, as is the case in the outer parts of the supercritical core, the expressions in equations (11) and (17) differ, and magnetic tension can indeed “overwhelm” self-gravity. This should clarify the issue raised in the footnote on p. 248 of LS.

compare very favorably with detailed numerical simulations.<sup>6</sup> Specifically, the only initial surface-density and magnetic-field distributions that are consistent with a self-similar evolution are

$$\sigma(r, 0) \propto B_z(r, 0) = B_{r,s}(r, 0) \propto \frac{1}{r}. \quad (20)$$

For these distributions the initial mass-to-flux ratio is constant throughout the disk:<sup>7</sup>

$$\frac{\sigma(r, 0)}{B_z(r, 0)} \equiv \frac{\lambda_o}{2\pi G^{1/2}} = \text{const.} \quad (21)$$

As it turns out, the scalings given by equation (20) are indeed representative of the central region of a collapsing core at the time of point-mass formation (see CM94, CM95, BM94, BM95a,b, and Basu 1997). We therefore associate that instant with the time  $t = 0$ , and, adopting the nomenclature introduced by Li & Shu (1996), we denote the corresponding disk configuration as the “pivotal” state of the model.

We emphasize once again the point first made in §1 that the pivotal state is *not* the end state of the sequence of subcritical quasi-static equilibria that slowly evolve due to ambipolar diffusion.<sup>8</sup> In fact, our pivotal state represents a dynamically collapsing disk with

$$\dot{M}(r, 0) \neq 0, \quad u(r, 0) \neq 0. \quad (22)$$

A simple physical argument clarifies why the self-similar pivotal state cannot correspond to hydrostatic equilibrium when ambipolar diffusion is self-consistently taken into account. Self-similarity requires a nonuniform distribution of  $B_z$  at  $t = 0$  (eq. [20]), which, in order to be supported, requires a *nonzero (and positive) drift speed*  $u_D$  between ions and neutrals (eq. [10]); otherwise  $B_{r,s}(r, 0)$  would have been zero and  $B_z(r, 0)$  would have been uniform, which is clearly not the case. During the initial phase of core collapse ( $t \leq 0$ ) the magnetic flux either remains fixed in space or else is advected inward, i.e.  $u_i(r, t \leq 0) \lesssim 0$ . Hence

$$|u(r, 0)| \equiv |u_i(r, 0) - u_D| \gtrsim u_D = C \frac{\eta}{\lambda_o^2} \left(1 + \frac{h}{r}\right), \quad (23)$$

---

<sup>6</sup>Note that, although the numerical models exhibit a self-similar behavior at late times irrespective of the detailed early-time ( $t \rightarrow -\infty$ ) conditions, only one particular set of distributions corresponds to exact self-similarity at  $t = 0$ .

<sup>7</sup>LS refer to disks in which the mass-to-flux ratio is a spatial constant as being *isopedic*.

<sup>8</sup>It is interesting to note, however, that our  $t = 0$  surface-density and magnetic field distributions (eq. [20]) are the same as those of the static pivotal state in the LS similarity solution, which corresponds to a singular isothermal disk (see Li & Shu 1996).

where the expression for  $u_D$  follows from equations (2), (10), (20), and (21). One can obtain an order-of-magnitude estimate for  $\dot{M}(r, 0)$  by using also equation (4) to approximate  $\sigma(r, 0)$  by its value in equilibrium,

$$\sigma(r, 0) \approx \frac{C^2}{2\pi Gr} \left( \frac{\lambda_o^2 + 2}{\lambda_o^2 - 1} \right), \quad u_D \approx \frac{3\eta C}{(\lambda_o^2 + 2)}, \quad \text{and} \quad \dot{M}(r, 0) \approx \frac{C^3}{G} \frac{3\eta}{(\lambda_o^2 - 1)}. \quad (24)$$

Taking as representative values  $\lambda_o = 2.9$  and  $\xi_{-17} = 5$  (see §3.4), one infers

$$|u(r, 0)| \gtrsim 0.1C \quad \text{and} \quad \dot{M}(r, 0) \approx 0.2 \left( \frac{T}{10 \text{ K}} \right)^{3/2} \text{M}_\odot \text{ per } 10^6 \text{ yr}, \quad (25)$$

where  $T$  is the temperature. The numerical simulations of CK suggest that, in fact,  $|u(r, 0)| \gg u_D$ , and that  $\dot{M}(r, 0)$  is of the order of a few solar masses per  $10^6$  years.<sup>9</sup>

### 3.2. Dimensionless Equations

We start by introducing a similarity variable  $x$  and dependent nondimensional variables  $\hat{h}(x)$ ,  $a(x)$ ,  $v(x)$ ,  $g(x)$ ,  $m(x)$ ,  $\dot{m}(x)$ ,  $\mathbf{b}(x)$ , and  $\psi(x)$ :

$$x = r/Ct, \quad (26)$$

$$h = Ct \hat{h}(x), \quad \sigma(r, t) = [C/(2\pi Gt)] a(x), \quad u(r, t) = C v(x), \quad g_r = (C/t) g(x), \quad (27)$$

$$M(r, t) = (C^3 t/G) m(x), \quad \dot{M}(r, t) = (C^3/G) \dot{m}(x), \quad (28)$$

$$\mathbf{B} = (C/[G^{1/2}t]) \mathbf{b}(x), \quad \Psi(r, t) = (2\pi C^3 t/G^{1/2}) \psi(x), \quad (29)$$

where

$$m(x) = \int_0^x a(x') x' dx', \quad \dot{m}(x) = -axv, \quad \psi(x) = \int_0^x b_z(x') x' dx'. \quad (30)$$

In these variables, equations (3)–(5) and (1) can be rewritten as

$$\frac{da}{dx} = \frac{a}{1 - (x - v)^2} \left[ g + \frac{b_z}{a} \left( b_{r,s} - \hat{h} \frac{db_z}{dx} \right) + \frac{(x - v)^2}{x} \right] \quad (31)$$

$$\frac{dv}{dx} = (x - v) \frac{d \ln a}{dx} + \frac{x - v}{x}, \quad (32)$$

$$\psi = x(x - v)b_z - x\eta \left( \frac{b_z}{a} \right)^2 \left( \frac{a\hat{h}}{2} \right)^{1/2} \left( b_{r,s} - \hat{h} \frac{db_z}{dx} \right), \quad (33)$$

$$\hat{h} = \frac{ax^3}{2m_c} \left[ -1 + \left( 1 + \frac{8m_c}{a^2 x^3} \right)^{1/2} \right], \quad (34)$$

---

<sup>9</sup>Note that, for a 10 K  $H_2$  gas with an interstellar He abundance,  $m_n = 2.33$  a.m.u. and  $C^3/G = 1.58 \text{ M}_\odot \text{ per } 10^6 \text{ yr}$ .

where

$$g = -\frac{1}{x^2} \int_0^\infty x' a(x') \mathcal{K}(x'/x) dx' , \quad b_{r,s} = \frac{1}{x^2} \int_0^\infty x' b_z(x') \mathcal{K}(x'/x) dx' , \quad (35)$$

and  $m_c \equiv m(0)$ . These equations are integrated subject to the initial conditions

$$a \rightarrow \frac{A}{x} , \quad b_z \rightarrow \frac{a}{\lambda_o} , \quad v \rightarrow v_o , \quad \dot{m} \rightarrow A v_o \equiv \dot{m}_o \quad \text{as } x \rightarrow +\infty . \quad (36)$$

Since the value ( $m_c$ ) of the central point mass is not known a priori, the solution requires a numerical iteration to calculate  $\hat{h}$ .

The complicated expressions for  $g$  and  $b_{r,s}$  in equation (35) can in principle be solved by means of an iterative procedure. As noted by LS, it is natural to start such an iteration using the monopole terms

$$g \approx -\frac{m}{x^2} , \quad b_{r,s} \approx \frac{\psi}{x^2} , \quad (37)$$

where, by virtue of equation (15),  $m(x)$  satisfies

$$m = x(x - v)a . \quad (38)$$

With these substitutions one can solve for  $a(x)$  and  $b_z(x)$ , and, in turn, use the latter distributions to improve the estimates for  $g(x)$  and  $b_{r,s}(x)$ . This procedure can be repeated until a good convergence is attained. As it turns out, the behavior of the disk at  $t \geq 0$  is already very well described by the monopole approximation, so, in what follows, we only use the monopole terms in deriving our solutions.

The system of equations (31)–(34) contains a singular line at the locus of points in the  $(x, -v)$  plane where

$$(x - v)^2 = 1 , \quad (39)$$

which corresponds to the sonic line. This result should be contrasted with the criticality condition for ideal MHD, which involves the magnetosonic speed instead of just the thermal sound speed (see §3.3). The mathematical reason for this difference is that magnetic diffusivity introduces derivatives of higher order than in ideal MHD (e.g., Ferreira & Pelletier 1995). There is also an interesting physical explanation of this result. In a magnetohydrodynamic flow, information propagates via magnetosonic and sonic waves. The critical surfaces that appear in steady-state problems can be thought of as being the relics of the time-dependent problem in which the various waves had sufficient time to propagate to the exterior boundaries and communicate the information associated with those boundaries to the whole flow (Blandford & Payne 1982). When diffusivity is present, the only waves that can survive propagation to and from infinity are the sonic waves (since the magnetosonic waves simply dissipate away): this is the physical reason why only the

sonic critical point appears in steady-state, diffusive MHD. The collapse problem that we have formulated, although time dependent, resembles a steady-state problem in this respect because of the restrictive assumption of self-similarity, which effectively combines time and space into a single variable. It therefore also involves the establishment of a critical surface, whose nature is determined by the above argument.

### 3.3. The Flux-Frozen Case

We first consider the ideal-MHD case  $\eta = 0$ , with  $v_o \neq 0$ . In this limit, one can rewrite equation (33) (using eqs. [30] and [32]) as

$$\frac{d \ln b_z}{dx} = \frac{d \ln a}{dx} , \quad (40)$$

which introduces a singular line in the  $(x, -v)$  plane given by

$$(x - v)^2 = 1 + 2\lambda^{-2} \quad (41)$$

(where, under the assumed ideal-MHD conditions, the mass-to-flux ratio  $\lambda = a/b_z$  is a constant). This singular line is *different* from the one given by equation (39) for the nonideal case. In physical units, equation (41) can be rewritten as  $r/t - u = \pm(C^2 + u_A^2)^{1/2}$ , where  $u_A \equiv B_z/(4\pi[\pi G\sigma^2/2C^2])^{1/2}$  and  $(C^2 + u_A^2)^{1/2}$  are, respectively, the effective Alfvén and magnetosonic speeds in the disk.<sup>10</sup> The equations now describe the  $t > 0$  collapse of an isothermal and isopedic disk with  $\lambda(x) = \lambda_o = \text{const}$ . The solution for the representative parameter set  $\lambda_o = 2.9$ ,  $-v_o = 1$ , and  $\dot{m}_o = 3$  (see §3.4) is shown in Figures 2a–2d. It is seen that, as the collapse progresses, mass accumulates at the origin at a rate

$$\dot{M}_c = 9.6 \left( \frac{T}{10 \text{ K}} \right)^{3/2} \text{ M}_\odot \text{ per } 10^6 \text{ yr} , \quad (42)$$

corresponding to  $m_c = 6.1$  in the expression

$$M_c(r = 0^+, t) = (C^3 t/G) m_c \quad (43)$$

for the central point mass. Note that, as discussed in connection with previous collapse calculations (see § 1), there is a significant and rapid increase ( $\dot{m}_c = 2.0 \dot{m}_o$ ) in the accretion

---

<sup>10</sup>When the density is given by  $\rho = \pi G\sigma^2/2C^2$  (see eq. [1]),  $u_A$  is equal to the usual Alfvén speed in the disk. The expression  $(C^2 + u_A^2/2)^{1/2}$  given by Shu & Li (1997, footnote 2) for the effective magnetosonic speed is evidently an error.

rate following point-mass formation. Near the origin, the flow proceeds in “diluted” free fall,

$$-v = [2m_c(1 - \lambda_o^{-2})/x]^{1/2}, \quad a = [m_c/2(1 - \lambda_o^{-2})x]^{1/2}, \quad \dot{m} = m_c. \quad (44)$$

The magnetic field advected to the center assumes a split-monopole topology,

$$b_z = \frac{a}{\lambda_o} \propto x^{-1/2}, \quad b_{r,s} = \frac{m_c}{\lambda_o x^2} \propto x^{-2}. \quad (45)$$

These results, obtained using the monopole approximation (eq. [37]), change little when one corrects for the deviations from the exact expressions for  $g$  and  $b_{r,s}$ . They differ from the ideal-MHD results presented in LS in that *the collapse occurs without discontinuities in the flow parameters or their derivatives*. The robustness of this conclusion is manifested by the fact that the solution curve in the  $(x, -v)$  plane never approaches too closely to the singular line. As we noted in §1, the initial state adopted by LS is characterized by  $v_o = 0$ : as a result, their integration from  $x = +\infty$  toward  $x = 0$  encounters the singular line. In order to form a point mass at the origin, they then need to connect to one of the “minus” solutions defined in Shu (1977). When they perform the integration in the monopole approximation, the connection takes place with continuous flow parameters (but discontinuous first derivatives) at the point where the singular line crosses the axis  $-v = 0$ . However, when they use more accurate expressions for  $g_r$  and  $B_{r,s}$ , the curve intersects the singular line a little bit below the axis  $-v = 0$ , where (according to Fig. 2 in Shu 1977) no “minus” solutions exist. In this case the connection to a “minus” solution can be achieved only through a discontinuous jump across the singular line, and this is the weak shock that LS invoke. Our solution demonstrates that such a shock is not required when  $v_o \neq 0$ . This result is confirmed by the flux-frozen collapse model presented in §3.3 of CK. (As discussed in § 1, numerical simulations of nonmagnetic collapse have shown that the Larson-Penston 1969 solution, which also has  $v_o \neq 0$ , provides an accurate approximation to the physical state at the instant of PMF in unmagnetized clouds.)

### 3.4. The Ambipolar-Diffusion Shock

We now proceed to derive the solution for the realistic, nonideal case (i.e.,  $\eta \neq 0$  for  $x \geq 0$ ). We continue to employ the monopole approximation for the gravity and magnetic field, which we subsequently justify both by verifying that the correction terms remain small and by comparing the results with the CK numerical simulations. One immediately realizes that the split-monopole field topology (eq. [45]) that characterizes the ideal-MHD solution near the origin cannot apply in the presence of ambipolar diffusion. This is because, for the split monopole,  $b_{r,s} \propto x^{-2} \gg b_z \propto x^{-1/2}$  as  $x \rightarrow 0^+$ , so the diffusive term in the

induction equation (eq. [5]) greatly exceeds the advective term near the origin. In practice, the outward diffusion prevents the formation of the split monopole field configuration in the first place, and a *different* solution is established near the origin. This solution is characterized by the magnetic flux being left behind while matter continues to fall into the center and forms there a point mass that grows with time according to equation (43). The flow consequently turns into an “undiluted” free fall at small  $x$ ,

$$-v = 2a = (2m_c/x)^{1/2}, \dot{m} = m_c, \quad (46)$$

with corresponding field components

$$b_z = b_{r,s} = \frac{2^{1/4}m_c^{3/4}}{\eta^{1/2}x}. \quad (47)$$

In this case, although the magnetic field grows with decreasing distance from the origin, the magnetic force remains negligible in comparison with the gravitational pull of the central point mass. Equations (46) and (47) also demonstrate the interesting fact that the local (differential) mass-to-flux ratio  $\lambda = a/b_z \propto x^{1/2} \rightarrow 0$  as  $x \rightarrow 0^+$ . However, the ratio of the spatially integrated mass and flux diverges as the origin is approached, consistent with the physical picture of mass accumulating at the center after decoupling from the magnetic field.

Under the flux-freezing conditions of ideal MHD,  $\lambda(x) = \text{const.}$  (see §3.3). It may at first seem counterintuitive that, in the nonideal case, the local mass-to-flux ratio decreases with decreasing  $x$ , since one could expect ambipolar diffusion to become progressively more efficient at loading magnetic field lines with matter as one approached the densest parts of the core near the center. Indeed, this is what happens *before* point-mass formation (e.g., CM94; CM95). However, *after* PMF the center acts as a sink of matter, so the magnetic field lines become increasingly depleted of mass as one gets closer to the origin (although the integrated mass-to-flux ratio  $m/\psi$  does increase with decreasing  $x$ ).

Our numerical procedure for obtaining the solution in this case has been to integrate the differential equations inward and outward from an intermediate point near the origin, connecting them to the free-fall solution (eqs. [46] and [47]) at small  $x$  and to the pivotal state (eq. [36]) at large  $x$ . Figures 2e–2h show the derived solution for the parameter set  $\lambda_o = 2.9$ ,  $-v_o = 1.0c$ ,  $\xi_{-17} = 5$ , and  $\dot{m}_o = 3$ . These parameter values are typical of the outer layers of a supercritical core in the CK simulations and are consistent with physical quantities deduced from observations of protostellar cores (e.g., Crutcher et al. 1993, 1994). It is seen that, while the solution is everywhere continuous, it exhibits an abrupt change in the flow parameters at a certain value of  $x$ . This transition, which is characterized by a continuous evolution of the physical parameters, a neutral flow velocity that remains

supersonic throughout, and a faster deceleration of the ions than of the neutrals, represents a *C*-shock (e.g., Draine & McKee 1993, Smith & Mac Low 1997). A similar ambipolar diffusion-induced C-shock has been found in the numerical simulations of CK (see §4 for a detailed comparison between the self-similar solution and the CK results). We identify the position of the shock with the location of the abrupt drop in the ion velocity and determine the shock speed from the motion of this transition relative to the origin. The numerical integration yielded  $x_{\text{sh}} = v_{\text{sh}} = 0.3$  and  $\dot{m}_c = 5.9$ , or, equivalently,

$$\begin{aligned} r_{\text{sh}} &= 119 \left( \frac{T}{10 \text{ K}} \right)^{1/2} \left( \frac{t}{10^4 \text{ yr}} \right) \text{ AU}, \\ u_{\text{sh}} &= 0.06 \left( \frac{T}{10 \text{ K}} \right)^{1/2} \text{ km s}^{-1}, \\ \dot{M}_c &= 9.3 \left( \frac{T}{10 \text{ K}} \right)^{3/2} \text{ M}_\odot \text{ per } 10^6 \text{ yr}. \end{aligned} \quad (48)$$

As an aid in visualizing this self-similar solution, we present in Figure 3 time sequences of the disk density and radial velocity during the collapse up to the time when a  $1.1 M_\odot$  star is assembled at the center.

It is worth emphasizing that the C-shock we have found is *required* by ambipolar diffusion and *is not* the shock discussed in LS (which, as we pointed out in §3.3, is avoided altogether in an isopedic disk that has a nonzero initial infall velocity). In the present (diffusive) case the magnetic field cannot remain attached to the matter as mass starts to accumulate in the origin, so the field decouples from the gas as soon as a point mass appears at the center.<sup>11</sup> The region of decoupled flux grows outward at a fraction of the speed of sound and a C-shock develops at its outer boundary. An interesting and somewhat counterintuitive result is that the accretion rate onto the central point mass is *smaller* (albeit only slightly) in the case with ambipolar diffusion than in the flux-frozen case (compare Figs. 2d and 2h). The reason is that, as we have noted, the local mass-to-flux ratio decreases when the magnetic field decouples from the matter. The corresponding increase in the magnetic force slows down the inflow and thereby reduces the inflow rate. Note that the two components of the magnetic force, the field tension and the field pressure gradient, are everywhere of comparable magnitude, so one cannot neglect either of them in the analysis.

---

<sup>11</sup>This behavior can also be understood by comparing the ambipolar diffusion and gravitational contraction timescales, whose ratio after PMF decreases with diminishing distance from the origin — signaling the onset of dynamically important ambipolar diffusion on small scales — on account of the decrease in the free-fall time that is brought about by the mass accumulation at the center (see §1 and §3.3 in CK).

#### 4. Discussion

It is of interest to compare our self-similar model results with the detailed numerical simulations of CK. The model they present is of a  $\sim 5 M_{\odot}$  molecular cloud core with temperature  $T = 10$  K. Just prior to PMF ( $t \rightarrow 0^-$ ) the accretion rate is  $\dot{M} = 5.4 M_{\odot}$  per  $10^6$  yr and the mass-to-flux ratio at the center is  $\lambda = 3.6$  — note, however, that unlike the self-similar model, neither  $\dot{M}$  nor  $\lambda$  are uniform at that time in the model core of CK (see their Figs. 1c and 1h). Immediately after PMF the accretion rate rises to  $9.4 M_{\odot}$  per  $10^6$  yr, and it then decreases to  $5.6 M_{\odot}$  per  $10^6$  yr by the time a  $1 M_{\odot}$  protostar forms at the origin (which occurs at  $t = 1.5 \times 10^5$  yr). <sup>12</sup> Rapid ambipolar diffusion in the inner flux tubes halts the inward advection of magnetic flux, which piles up and propagates outward as a hydromagnetic disturbance. As the front of piled-up flux moves out to larger radii, the magnetic field behind the disturbance and the neutral–ion collisional coupling become strong enough to affect the infalling neutrals, and a shock forms in the core. The shock is of the C type (e.g., Mullan 1971; Draine 1980): the infall speed of the neutrals (in the shock frame) remains supersonic while the infall speed of the ions is much smaller than the ion Alfvén speed. By the time a  $1 M_{\odot}$  protostar has formed at the origin in their typical model calculation, the shock is located at a radius  $\sim 3.5 \times 10^3$  AU and propagates outward with a speed (in the stellar rest frame)  $\sim 0.7 C = 0.13$  km s $^{-1}$ . (For comparison, eq. [48] yields  $M_c \approx 1.4 M_{\odot}$ ,  $r_{sh} \approx 1.8 \times 10^3$  AU, and  $u_{sh} \approx 0.06$  km s $^{-1}$ , respectively, for the accumulated central mass, shock location, and shock speed at that time.) As the hydromagnetic disturbance propagates outward, the postshock accretion rate decreases due to the fact that the neutrals are “hung up” (i.e., decelerated) in the region of amplified magnetic field behind the shock front (see Fig. 6g of CK). This is also what happens in the self-similar model (Fig. 2h). As discussed in CK (see also Li & McKee 1996), the postshock region is potentially susceptible to interchange instabilities (i.e., the gravitationally-induced interchange of magnetic flux tubes; e.g., Spruit & Taam 1990; Spruit, Stehle, & Papaloizou 1995): this issue, however, cannot be fully addressed until nonaxisymmetric collapse simulations are performed.

In the limit  $r \rightarrow 0$  (or  $x \rightarrow 0$ ) the column density and the infall speed of the neutrals are both  $\propto r^{1/2}$  ( $\propto x^{1/2}$ , see eq. [46] and Figs. 2e, 2f, 3a, and 3b), reflecting the “undiluted” free-fall collapse induced by the central point mass. A similar behavior is also revealed in the numerical simulations (see Figs. 6c and 6e of CK).

---

<sup>12</sup>This time is equal to  $1.1 \tau_{gr}$ , where  $\tau_{gr} = [r_{M_{\odot}}^3/GM_{\odot}]^{1/2}$  is the gravitational contraction ( $\approx$  free-fall) time at the location  $r_{M_{\odot}}$  within the core, which contains  $1 M_{\odot}$  at  $t = 0$ . This result is similar to that observed in the nonmagnetic collapse solutions of Shu (1977), Hunter (1977), and Foster & Chevalier (1993).

As mentioned in §3.4, ambipolar diffusion “unloads” the mass in the effectively stationary (see Fig. 2e) flux tubes behind the shock front. As a result, the local mass-to-flux ratio  $\lambda(x) = a(x)/b_z(x)$  is no longer a monotonically decreasing function behind the shock (see Figs. 2f, 2g, and 3b); this behavior is also seen in the CK simulations (see their Fig. 8a).

One obvious advantage of the simple self-similar model is that one can scan the space of model parameters much more easily than is possible in the case of the time-consuming numerical simulations. For instance, the typical model presented in CK took  $\sim$  two weeks of computer time (running in background on an SGI R-4000 Indigo workstation) for the central mass to accumulate  $1M_\odot$  of material. By contrast, calculation of our self-similar models is usually completed within half a minute (for typical models) when run on the same workstation.

We note that Li & McKee (1996) suggested that Ohmic dissipation [a process that, for the assumed cloud composition and cosmic ray ionization rate, becomes important for densities  $n \gtrsim 10^{11} \text{ cm}^{-3}$  (e.g., Nakano & Umebayashi 1986a,b), or, equivalently, on scales  $r \ll 1 \text{ AU}$ ] would halt the accretion of flux onto a protostar, with the flux consequently presenting an obstacle to the neutrals and thereby giving rise to a shock. However, as shown by CK and verified by our self-similar model, ambipolar diffusion is sufficiently efficient at much lower densities (or much larger radii) to halt flux advection and cause the formation of a hydromagnetic shock, independent of the effect of Ohmic dissipation. Despite the misidentification of the shock formation mechanism and the fact that the induction equation was not solved for the magnetic field structure, the simplified model of Li & McKee was found by CK to provide a reasonably good approximation to the results of their numerical simulations.

As we have already noted in §3.1, the numerical results of core collapse and point-mass formation presented in CK can be described by a self-similar model only in an approximate sense. In particular, the condition of the spatial uniformity of  $u$ ,  $\dot{M}$ , and  $\lambda$  at the instant of PMF, as well as the scaling  $n_i \propto n^{1/2}$ , are generally not strictly valid in the cores of the models presented in CM94, CM95, BM94–BM95b, and CK. Furthermore, the temporal behavior of the physical quantities in our self-similar solution deviates from that in CK. For example, CK find that in the region of free-fall collapse near the central point mass  $-0.76 < d \ln \sigma / d \ln t < -0.55$ , which is different from the self-similar result  $d \ln \sigma / d \ln t = -1/2$  (see eqs. [27] and [46]). It is worth stressing, however, that, in spite of these differences, the self-similar solution accurately describes the formation of an outward-propagating ambipolar-diffusion shock as well as the other basic characteristics of the evolution of a protostellar core during the post-PMF epoch. As discussed in CK, the

numerical simulations of this model are consistent with observations of accreting protostars. In particular, the inferred evolution of the mass accretion rate is similar to that deduced for the protostellar objects HL Tauri and L1551-IRS5, and the calculated magnetic field structure agrees with polarimetric observations of dense protostellar cores (see § 4.2 of CK).

## 5. Conclusion

In this paper we have presented a self-similar solution of the collapse of a magnetized molecular cloud core (assumed to also be nonrotating and isothermal) that, for the first time, incorporated the effects of ambipolar diffusion in a self-consistent manner. We have focused on the post-PMF (point-mass formation) phase of the collapse of a disk-like core, noting that Basu (1997) had previously explored the self-similar nature of the collapse before a central mass (i.e., a protostar) first appears at the origin. We clarified the distinction between the ideal and nonideal MHD cases by plotting the singular lines in the position–velocity space and showing that they correspond to different critical speeds (the magnetosonic speed and thermal sound speed in the ideal and nonideal problems, respectively). We obtained a solution for the ideal (flux-frozen) case that exhibits a split-monopole field topology near the center. This solution differs from the one obtained by Li & Shu (1997) in that it involves no shocks. We showed that the shock in the LS solution is a direct consequence of their assumption that the core at the time of PMF is described by a stationary density distribution (corresponding to a singular isothermal toroid), and we pointed out that a shock will generally *not* be present under the more realistic assumption of a nonzero inflow speed near the origin at that instant. We demonstrated, however, that a shock is a generic feature of the solution in the nonideal (ambipolar diffusion) case. This (C-type) shock is a direct consequence of the action of ambipolar diffusion in the central region of the core following PMF: the magnetic diffusivity decouples the field from the matter, causing the gas to free-fall to the center (where it accumulates in a point mass) and the field to stay behind and drive a shock outward. We have compared this solution with the results of the numerical simulations of Ciolek & Königl (1998) and confirmed that, while the more realistic numerical models are not strictly self-similar, our simplified solution nevertheless captures the main features of the core evolution after PMF.

This work was supported in part by NASA grants NAG 5-2766 and NAG 5-3687. Helpful comments by the referee, Prudence Foster, are gratefully acknowledged.

## REFERENCES

Abramowitz, M., & Stegun, I. A. 1965, Handbook of Mathematical Functions (New York: Dover)

Basu, S. 1997, *ApJ*, 485, 240

Basu, S., & Mouschovias, T. Ch. 1994, *ApJ*, 432, 720 (BM94)

\_\_\_\_\_. 1995a, *ApJ*, 452, 386 (BM95a)

\_\_\_\_\_. 1995b, *ApJ*, 453, 271 (BM95b)

Blandford, R. D., & Payne, D. G. 1982, *MNRAS*, 199, 883

Boss, A. P., & Black, D. C. 1982, *ApJ*, 258, 270

Chiueh, T., & Chou, J.-K. 1994, *ApJ*, 431, 380

Ciolek, G. E., & Königl, A. 1998, *ApJ*, in press (CK)

Ciolek, G. E., & Mouschovias, T. Ch. 1993, *ApJ*, 418, 774 (CM93)

\_\_\_\_\_. 1994, *ApJ*, 425, 142 (CM94)

\_\_\_\_\_. 1995, *ApJ*, 454, 194 (CM95)

\_\_\_\_\_. 1998, *ApJ*, in press

Crutcher, R. M., Mouschovias, T. Ch., Troland, T. H., & Ciolek, G. E. 1994, *ApJ*, 427, 839

Crutcher, R. M., Troland, T. H., Goodman, A. A., Heiles, C., Kazés, I., & Myers, P. C. 1993, *ApJ*, 407, 175

Dalgarno, A. 1987, in Physical Processes in Interstellar Clouds, ed. G. E. Morfill & M. Scholer (Dordrecht: Reidel), 219

Draine, B. T. 1980, *ApJ*, 241, 1021

Draine, B. T., & McKee, C. F. 1993, *ARA&A*, 31, 373

Elmegreen, B. G. 1979, *ApJ*, 232, 729

Ferreira, J., & Pelletier, G. 1995, *A&A*, 295, 807

Fiedler, R. A., & Mouschovias, T. Ch. 1992, *ApJ*, 391, 199

\_\_\_\_\_. 1993, *ApJ*, 415, 680

Foster, P. C., & Chevalier, R. A. 1993, *ApJ*, 416, 303

Galli, D., & Shu, F. H. 1993a, *ApJ*, 417, 220

\_\_\_\_\_. 1993b, *ApJ*, 417, 243

Gaustad, J. E. 1963, *ApJ*, 138, 1050

Henriksen, R. N. 1994, in The Cold Universe, ed. T. Montmerle, C. J. Lada, I. F. Mirabel, & J. Trần Thanh Vân (Editions Frontières), 241

Hildebrand, R. H., Dragovan, M., & Novak, G. 1984, *ApJ*, 284, L51

Hunter, C. 1977, *ApJ*, 218, 834

Kane, B. D., Clemens, D. P., Barvainis, R., & Leach, R. W. 1993, *ApJ*, 411, 708

Larson, R. B. 1969, *MNRAS*, 145, 271

Li, Z.-Y., & McKee, C. F. 1996, *ApJ*, 64, 373

Li, Z.-Y., & Shu, F. H. 1996, *ApJ*, 472, 211

\_\_\_\_\_. 1997, *ApJ*, 475, 237 (LS)

Matsumoto, T., Hanawa, T., & Nakamura, F. 1997, *ApJ*, 478, 569

McDaniel, E. W., & Mason, E. A. 1973, The Mobility and Diffusion of Ions and Gases (New York: Wiley), 282

Mouschovias, T. Ch. 1987, in Physical Processes in Interstellar Clouds, ed. G. Morfill & M. Scholer (Dordrecht: Reidel), 453

Mullan, D. J. 1971, *MNRAS*, 153, 145

Nakamura, F., Hanawa, T., & Nakano, T. 1995, *ApJ*, 444, 770

Nakano, T., & Umebayashi, T. 1986a, *MNRAS*, 218, 663

\_\_\_\_\_. 1986b, *MNRAS*, 221, 319

Narita, S., Hayashi, C., & Miyama, S. M. 1984, *Prog. Theor. Phys.*, 72, 118

Novak, G., Predmore, C. R., & Goldsmith, P. F. 1990, *ApJ*, 355, 166

Penston, M. V. 1969, *MNRAS*, 144, 425

Pneuman, G. W., & Mitchell, T. P. 1965, *Icarus*, 4, 494

Safier, P. N., McKee, C. F., & Stahler, S. W. 1997, *ApJ*, 485, 660

Shu, F. H. 1977, *ApJ*, 214, 488

Shu, F. H., Adams, F. C., & Lizano, S. 1987, *ARA&A*, 25, 23

Shu, F. H., & Li, Z.-Y. 1997, *ApJ*, 475, 251

Smith, M. D., & Mac Low, M.-M. 1997, *A&A*, 326, 801

Spruit, H. C., Stehle, R., & Papaloizou, J. C. B. 1995, *MNRAS*, 275, 1223

Spruit, H. C., & Taam, R. E. 1990, *A&A*, 229, 475

Tsai, J. C., & Hsu, J. J. L. 1995, *ApJ*, 448, 774

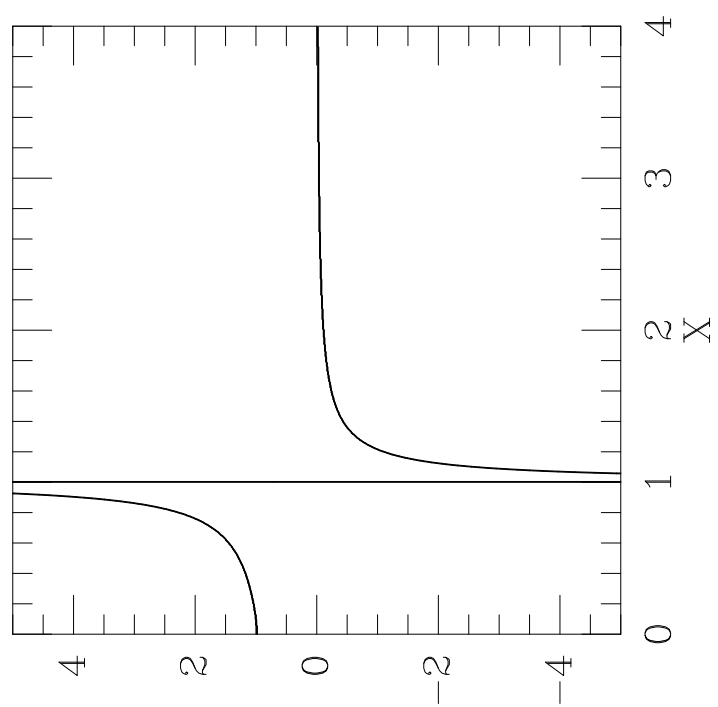
Watson, W. D. 1976, Rev. Mod. Phys., 48, 513  
Whitworth, A. P., & Summers, D. 1985, MNRAS, 214, 1

### Figure Captions

**Fig. 1.**—A plot of the function  $\mathcal{R}(X)$ , which determines how different disk radii are weighted in the expressions for the gravitational acceleration (eq. [11]) and the surface radial magnetic field (eq. [18]). The function is normalized by  $\int_0^\infty \mathcal{R}(X) dX = 1$ .

**Fig. 2.**—Self-similar collapse solutions for an ideal-MHD ( $\eta = 0$ ) disk (a) – (d) and for an ambipolar diffusion-dominated ( $\eta = 0.3$ ) disk (e) – (h), for initial conditions represented by the parameters  $v_o = -1.0$ ,  $\lambda_o = 2.9$ , and  $\dot{m}_o = 3$ . Plotted as a function of the similarity variable  $x$  are the radial speeds (in units of the speed of sound  $C$ ) of the neutrals ( $v$ , *solid curve*) and ions ( $v_i$ , *dashed curve*) in panels (a) and (e), the dimensionless surface density  $a$  in panels (b) and (f), the normalized vertical ( $b_z$ , *solid curve*) and radial surface ( $b_{r,s}$ , *dashed curve*) magnetic field components in panels (c) and (g), and the mass accretion rate into the center ( $\dot{M}$ , for a temperature  $T = 10$  K) in panels (d) and (h). Note that the ions comove with the neutrals in the ideal-MHD case (panel [a]). The singular curves (*open circles*) in panels (a) and (e) correspond to straight lines in nonlogarithmic units [ $x - v = (1 + 2\lambda_o^{-2})^{-2}$  in the ideal-MHD case and  $x - v = 1$  in the presence of ambipolar diffusion]. Both solutions are continuous and have supersonic neutral speeds for all  $x$ . The abrupt ion deceleration in the nonideal solution gives rise to a strong C-shock. No shock appears in the ideal solution. At large  $x$  (equivalently, large  $r$ ),  $v \rightarrow \text{const.}$  and  $a \propto b_z \approx b_{r,s} \propto x^{-1}$ . At small  $x$  (equivalently, small  $r$ ), the diffusive solution differs from the ideal-MHD one. Both solutions contain a point mass at the center and therefore both exhibit free-fall-type profiles ( $v \propto a \propto x^{-1/2}$ ) near the origin. However, the nonideal solution has  $b_z \approx b_{r,s} \propto x^{-1}$ , whereas the ideal-MHD one ( $b_z \propto a$ ) contains a split magnetic monopole at the center ( $b_z \propto x^{-1/2}$  and  $b_{r,s} \propto x^{-2}$ ).

**Fig. 3.**— The distributions of the core infall speed  $u$  and surface number density  $N$  at times  $t = 0, 2, 4, 6, 8, 10$ , and  $12 \times 10^4$  yr *after* a point mass forms at the center. By the end of the displayed evolution, 1.1 solar masses have accumulated at the origin.



$$R(X)$$

Fig. 1.—

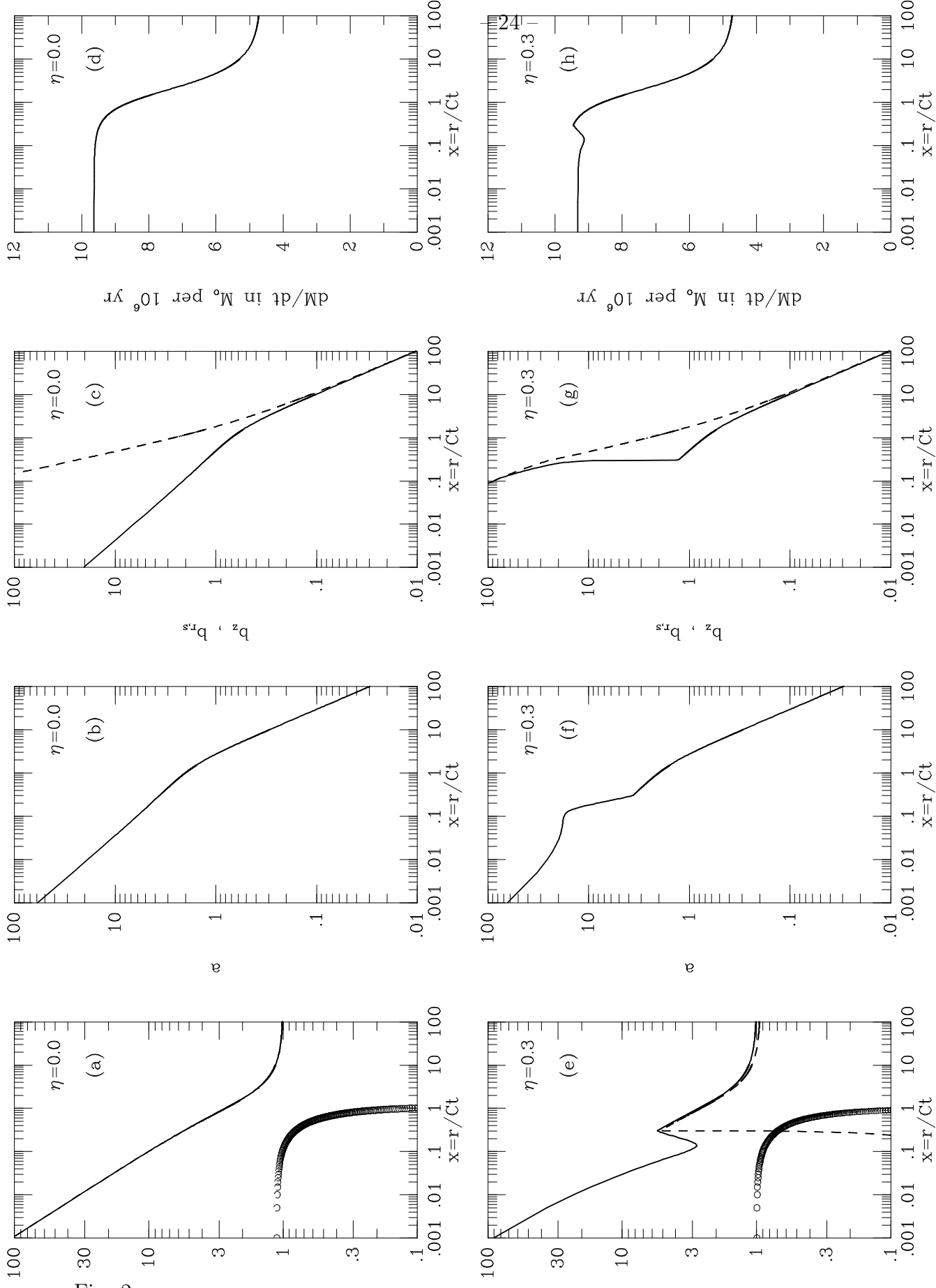


Fig. 2.—

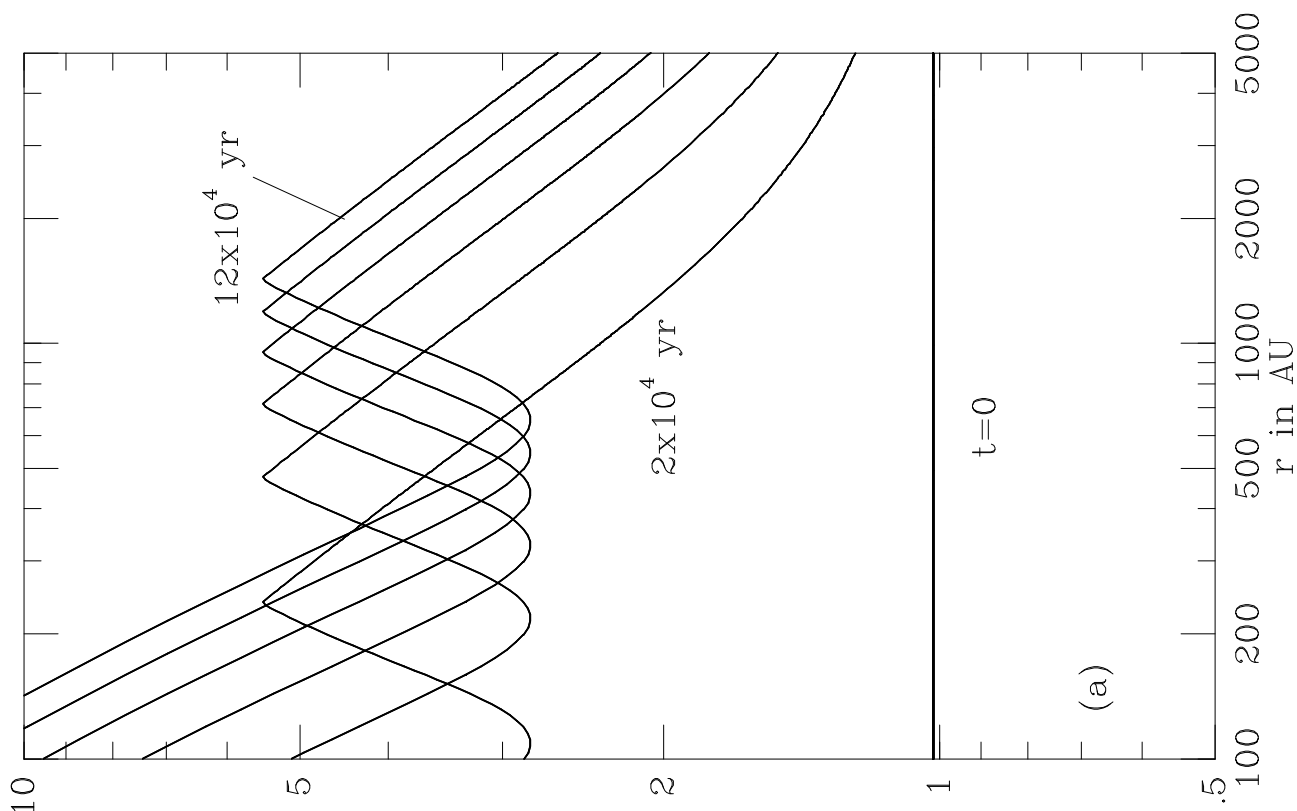
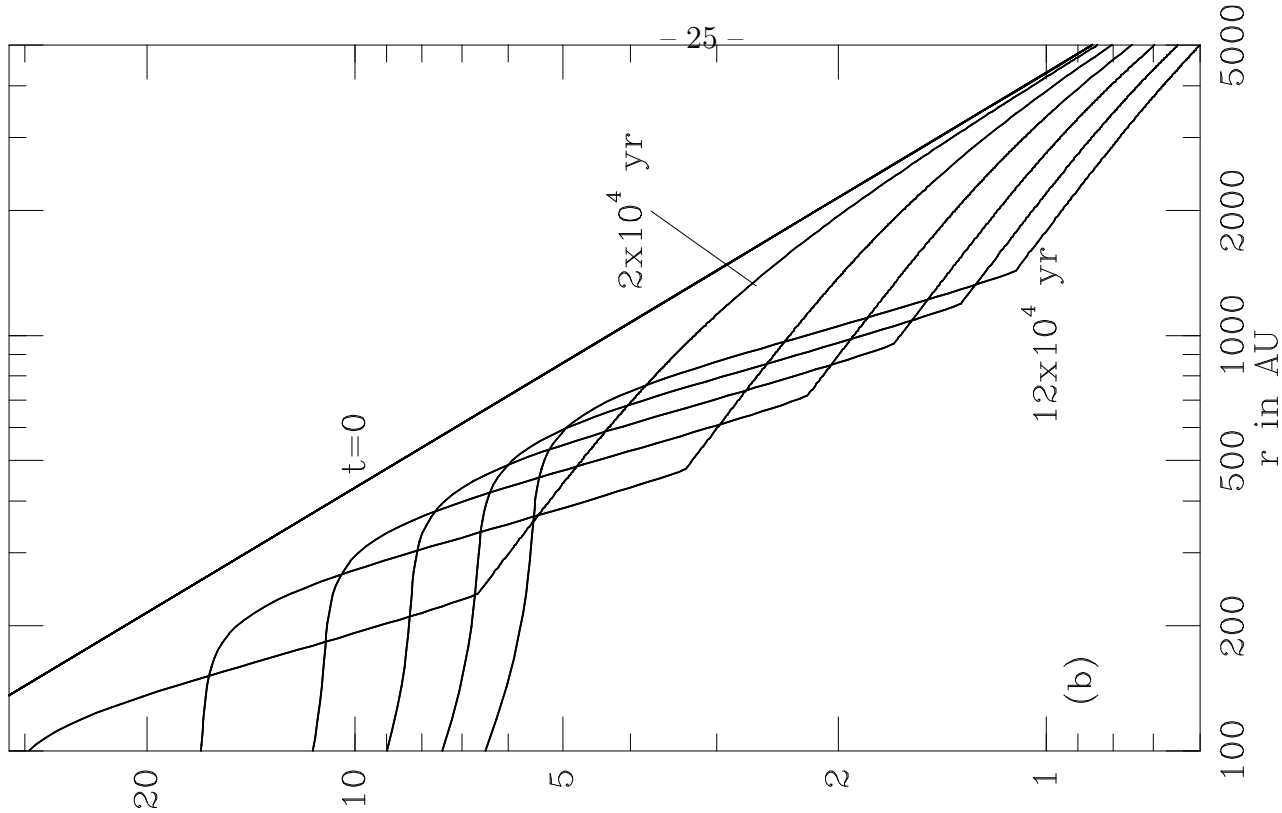


Fig. 3.—

$-u/c$